

## Article

# Sustainable Aromatic Production from Catalytic Fast Pyrolysis of 2-Methylfuran over Metal-Modified ZSM-5

Shengpeng Xia<sup>1,2,3,4</sup>, Chenyang Wang<sup>1,2,3,4</sup>, Yu Chen<sup>1,2,3,5</sup>, Shunshun Kang<sup>1,2,3,4</sup>, Kun Zhao<sup>1,2,3,5,\*</sup>, Anqing Zheng<sup>1,2,3,5,\*</sup>, Zengli Zhao<sup>1,2,3,5</sup> and Haibin Li<sup>1,2,3,4</sup>

<sup>1</sup> Guangzhou Institute of Energy Conversion, Chinese Academy of Sciences, Guangzhou 510640, China

<sup>2</sup> CAS Key Laboratory of Renewable Energy, Guangzhou 510640, China

<sup>3</sup> Guangdong Provincial Key Laboratory of New and Renewable Energy Research and Development, Guangzhou 510640, China

<sup>4</sup> University of Chinese Academy of Sciences, Beijing 100049, China

<sup>5</sup> School of Energy Science and Engineering, University of Science and Technology of China, Guangzhou 510640, China

\* Correspondence: zhaokun@ms.giec.ac.cn (K.Z.); zhengaq@ms.giec.ac.cn (A.Z.);

Tel.: +86-0208-7057-716 (K.Z. & A.Z.); Fax: +86-0208-7057-737 (K.Z. & A.Z.)

**Abstract:** The catalytic fast pyrolysis (CFP) of bio-derived furans offers a promising approach for sustainable aromatic production. ZSM-5 modified by different metal species (Zn, Mo, Fe, and Ga) was employed in the CFP of bio-derived furans for enhancing aromatic production. The effects of metal species, metal loadings, and the weight hourly space velocity (WHSV) on the product distributions from the CFP of 2-methylfuran (MF) were systemically investigated. It is found that the introduction of Zn, Mo, Fe, and Ga on ZSM-5 significantly increases the MF conversion and aromatic yields. The maximum MF conversions of 75.49 and 69.03% are obtained, respectively, by Fe-ZSM-5 and Ga-ZSM-5, which boost the aromatic yield by 34.5 and 42.7% compared to ZSM-5. The optimal loading of Fe on ZSM-5 is 2%. Additionally, the highest aromatic yield of 40.03% is achieved by 2%Fe-ZSM-5 at a WHSV of 2 h<sup>-1</sup>. The catalyst characterization demonstrates that the synergistic effect of Brønsted and Lewis acid sites in Fe-ZSM-5 is responsible for achieving the efficient aromatization of MF. The key to designing improved zeolite catalysts for MF aromatization is the introduction of large numbers of new Lewis acid sites without a significant loss of Brønsted acid sites in ZSM-5. These findings can provide guidelines for the rational design of better zeolite catalysts used in the CFP of biomass and its derived furans.

**Keywords:** biomass; bio-derived furan; aromatization; ZSM-5; catalyst design



**Citation:** Xia, S.; Wang, C.; Chen, Y.; Kang, S.; Zhao, K.; Zheng, A.; Zhao, Z.; Li, H. Sustainable Aromatic Production from Catalytic Fast Pyrolysis of 2-Methylfuran over Metal-Modified ZSM-5. *Catalysts* **2022**, *12*, 1483. <https://doi.org/10.3390/catal12111483>

Academic Editors: Chuande Huang, Bo Jiang, Xin Tian and Jiawei Hu

Received: 2 November 2022

Accepted: 16 November 2022

Published: 20 November 2022

**Publisher's Note:** MDPI stays neutral with regard to jurisdictional claims in published maps and institutional affiliations.



**Copyright:** © 2022 by the authors. Licensee MDPI, Basel, Switzerland. This article is an open access article distributed under the terms and conditions of the Creative Commons Attribution (CC BY) license (<https://creativecommons.org/licenses/by/4.0/>).

## 1. Introduction

Nowadays, with increasing concerns regarding the upcoming scarcity of fossil fuel resources and the environmental issues associated with their usage, unequalled endeavors have been made to produce liquid fuels and chemicals from renewable energy resources [1–3]. Biomass is the only renewable resource capable of producing chemicals and liquid fuels [4]. Pyrolysis has been recognized as one of the most promising technologies that can yield diverse phase products comprising char, gas, and bio-oil from biomass [5–7]. However, bio-oil derived from biomass pyrolysis has a complex composition, low calorific value, high oxygen content, strong acidity, and poor stability, making it unsuitable for use in the current petroleum infrastructure. Multiple techniques have been applied to bio-oil upgrading, including raw material pretreatment, catalytic hydrodeoxygenation, and catalytic fast pyrolysis (CFP). Recently, CFP of biomass has been extensively explored, seeking to selectively produce value-added chemicals from biomass, especially aromatics [8]. Monocyclic aromatics—namely, benzene, toluene, ethylbenzene, and xylene (BTEX)—are bulk

organic chemicals for the production of rubber, fibers, plastics, resins, coatings, dyes, pesticides, and pharmaceuticals [9]. In addition, they are also significant blending components of high-octane clean gasoline (accounting for around 21% of the gasoline composition) [10].

Previous studies have established that zeolite is the optimum catalyst for generating aromatics by the CFP of biomass due to its unique physicochemical features with acidity and pore structure. A succession of zeolite catalysts has been applied to the CFP of biomass, including HZSM-5, HY, H-beta, SAPO-34, MCM-41, etc. It has been proven that HZSM-5 has a moderate pore size and excellent shape selectivity for aromatics, whereas HY can accommodate more intermediate products. Xiangyu Li and coworkers observed that the CFP of Kraft lignin with HZSM-5 zeolite could produce a variety of valuable chemicals such as BTX, ethene, and propene [11]. Jae-Young Kim et al. examined the influence of the acidity of HZSM-5 on the production of aromatics from the pyrolysis of lignin. They found that the aromatic yield increased from 0.76% (Si/Al mole ratio of 280) to 2.62% (Si/Al mole ratio of 30) in proportion to increasing catalyst acidity [12]. Shanmugam Thiyagarajan et al. demonstrated that renewable aromatics may be synthesized from furans using HY zeolite, which exhibited the best activity and can be readily reused after calcination [13].

It was observed that transition-metal-modified zeolite catalysts may greatly boost monocyclic aromatic yields and facilitate the transformation of polycyclic aromatics into monocyclic aromatics. Evgeny A. Uslamin and coworkers reported a mechanistic investigation of the aromatization of furans over Ga-modified HZSM-5 [14–17]. They observed that the introduction of Ga can enhance aromatic selectivity and influence the deactivation pathway, leading to the formation of PAHs [17]. It has been reported that the addition of Fe into ZSM-5 zeolite contributed to the formation of MAHs and simultaneously hindered the further polymerization reaction of MAHs and other oxygenates during the catalytic fast pyrolysis of biomass [15]. As mentioned above, the introduction of transition metals can significantly increase aromatic yields. Here, transition-metal-modified HZSM-5 was applied to enhance the yield of aromatics.

Bio-derived furans, such as 2-methylfuran (MF), furfural, and 2,5-dimethylfuran, are key platform molecules obtained from the pyrolysis or hydrolysis of cellulose and hemicellulose, which have been widely used as the model compounds of cellulose and hemicellulose [18–30]. Yu-Ting Cheng and George W. Huber investigated the cofeeding of olefins (ethylene and propylene) with a series of furans over ZSM-5 catalysts and found that aromatics can be produced directly by Diels–Alder cycloaddition reactions of furans with olefins [22]. Huiyan Zhang et al. explored the catalytic conversion of furfural to olefins and aromatics and proposed a catalytic reaction pathway that starts with furfural decarboxylation to form furan and then form olefins and aromatics with further reactions [31]. However, there are relatively few studies on the production of aromatics by the pyrolysis of MF alone and the main pathway from furans to aromatics is through the Diels–Alder reaction [19,22,28]. Here, MF, a typical representative of bio-derived furans, is used as a model compound of cellulosic biomass.

In this work, the CFP of MF over ZSM-5 modified by different metals (Mo, Zn, Ga, and Fe) was carried out in a fixed bed reactor. In addition, different metal loadings and WHSVs were examined to further improve the catalytic performance. The metal-modified ZSM-5 catalysts were characterized to establish the structure-reactivity relationship.

## 2. Results and Discussion

### 2.1. The Product Distribution from the CFP of MF over ZSM-5 Modified by Different Metal Species

Figure 1 illustrates the MF conversion and carbon yields of BTEX, olefins, and coke from the CFP of MF over ZSM-5 modified by different metal species. It is observed that the introduction of four types of metal (Zn, Mo, Fe, and Ga) can significantly improve the conversion of MF and the carbon yield of BTEX and aromatics. Compared with raw ZSM-5 zeolite, metal-modified ZSM-5 zeolites can produce more alkanes, CO, and CO<sub>2</sub>, indicating that metal sites can efficiently promote the deoxygenation reactions of MF and

the formation of alkanes, primarily  $C_1$ – $C_3$ . However, the carbon yield of coke from the CFP of MF over ZSM-5 increases by metal modification, except for the Mo modification. The results could be due to the change in the acid amount of the ZSM-5 catalysts caused by metal modification. It is also observed that metal-modified ZSM-5 catalysts largely improve the carbon output of benzene and toluene, but the carbon yields of ethylbenzene and xylene change slightly. The maximum carbon yields of BTEX (23.6%) and aromatics (30.1%) are obtained by Ga-ZSM-5, whereas the maximum conversion of MF (75.5%) is obtained by Fe-ZSM-5, which provides the aromatic yield of 28.3%. The Fe and Ga modifications can boost the aromatic yield by 34.5 and 42.7% compared to raw ZSM-5. Interestingly, the highest carbon yield of alkylbenzene is gained over Fe-ZSM-5 and the highest carbon yield of benzene is gained over Ga-ZSM-5, demonstrating that Fe exhibits a stronger aromatization ability and Ga displays a better dealkylation ability. Meanwhile, Mo and Fe can promote the formation of olefins (primarily ethylene and propylene). It is noteworthy that when the metal loading increases from 1 to 4%, the carbon yields of BTEX, aromatics, and conversion of MF decrease. Similarly, Ga and Fe modification affords the highest MF conversion and aromatic yields. It is thus concluded that the loading of Zn, Mo, Fe, and Ga on ZSM-5 zeolite can effectively enhance the MF conversion and the yields of BTEX and aromatics. Fe- and Ga-modified ZSM-5 catalysts exhibit the maximum MF conversion and aromatic yield, respectively.

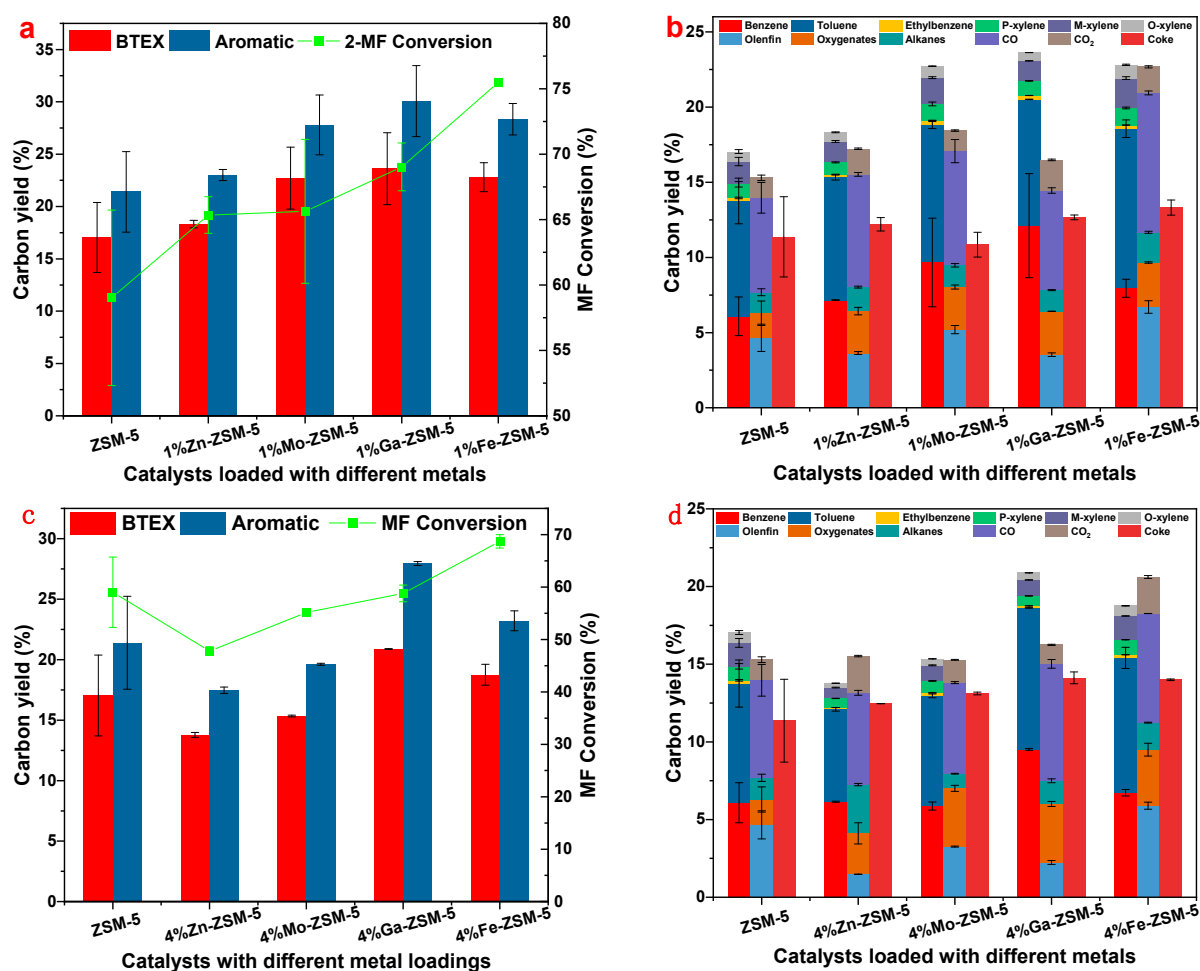


**Figure 1.** The effect of metal species on the product distribution from CFP of MF over metal-modified ZSM-5: (a,c) carbon yields of BTEX, aromatics, and MF conversion; (b,d) carbon yields of benzene, toluene, ethylbenzene, xylene, olefins, oxygenates, alkane, CO, CO<sub>2</sub>, and coke. Reaction conditions: 550 °C, WHSV: 4 h<sup>-1</sup>, carrier gas flow rate: 120 mL/min, reaction time: 15 min.

### 2.2. The Effect of Fe Loading on the Product Distribution from the CFP of MF over Fe-ZSM-5

Fe-ZSM-5 with different Fe loadings is employed in the CFP of MF since Fe-ZSM-5 exhibits the highest MF conversion among the four types of metal-modified ZSM-5. The resulting product distributions are shown in Figure 2. With the increase in Fe loading, the MF conversion and the carbon yields of BTEX, aromatics, and coke first increase and then reach their respective maximum values of 83.3%, 24.3%, 30.3%, and 15.7% at Fe loadings of 3%, 2%, 2%, and 3%. However, the MF conversion and the yield of aromatics and coke at an Fe loading of 0.5% are higher than those at an Fe loading of 1%. This may be owing to the high dispersion of Fe with a 0.5% loading forming more effective active sites. Simultaneously, the maximum yields of alkylbenzene, olefins, alkane, CO, and CO<sub>2</sub> are achieved at a 2% loading, indicating that 2% is optimum for the CFP of MF. As the Fe loading increases, the number of acid sites in the Fe-ZSM-5 catalyst increases, and the pores become blocked, so that the carbon yields of BTEX, aromatics, etc., begin to drop. Appropriate metal loading and metal dispersion not only improve product distribution but effectively reduce the consumption of metals.

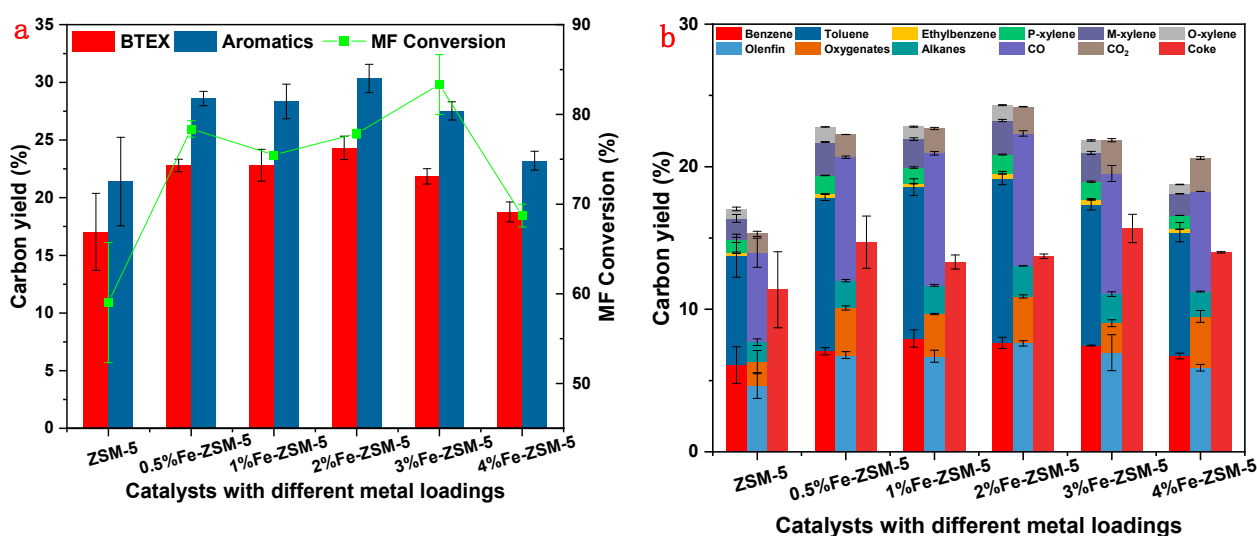


**Figure 2.** Effect of metal loadings on the product distribution from CFP of bio-derived MF: (a) carbon yields of BTEX, aromatics, and MF conversion; (b) carbon yields of benzene, toluene, ethylbenzene, xylene, olefins, oxygenates, alkane, CO, CO<sub>2</sub>, and coke. Reaction conditions: 550 °C, WHSV: 4 h<sup>-1</sup>, carrier gas flow rate: 120 mL/min, reaction time: 15 min.

### 2.3. The Effect of WHSV on the Product Distribution from the CFP of MF

Figure 3 showed the detailed product distribution from the conversion of MF at different WHSVs. The WHSV is defined as the mass flow rate of MF divided by the mass of the catalyst used in the reactor. In this experiment, the mass of the catalyst was altered from 0.5 to 2 g, while the mass flow rate of MF was maintained constant. As shown in Figure 3, the yields of BTEX, aromatics, olefins, and coke are a function of the WHSV. As the WHSV decreases from 8 h<sup>-1</sup> to 2 h<sup>-1</sup>, the yields of BTEX, aromatics, and coke increase from 9.23%, 11.72%, and 7.68% to 31.93%, 40.03%, and 23.69%, respectively, while the yield of olefins increases from 3.61% to 9.01%, and then remains unchanged. As indicated in Figure 3, the conversion of MF increases with decreasing WHSV and achieves 98.52% at a WHSV of 2 h<sup>-1</sup>. It is inferred that the increasing amount of catalyst used can provide more active sites for the aromatization reaction of MF, leading to an increase in MF conversion and aromatic yield. These findings reveal that the appropriate WHSV for the conversion of MF was less than or equal to 2.67 h<sup>-1</sup>.

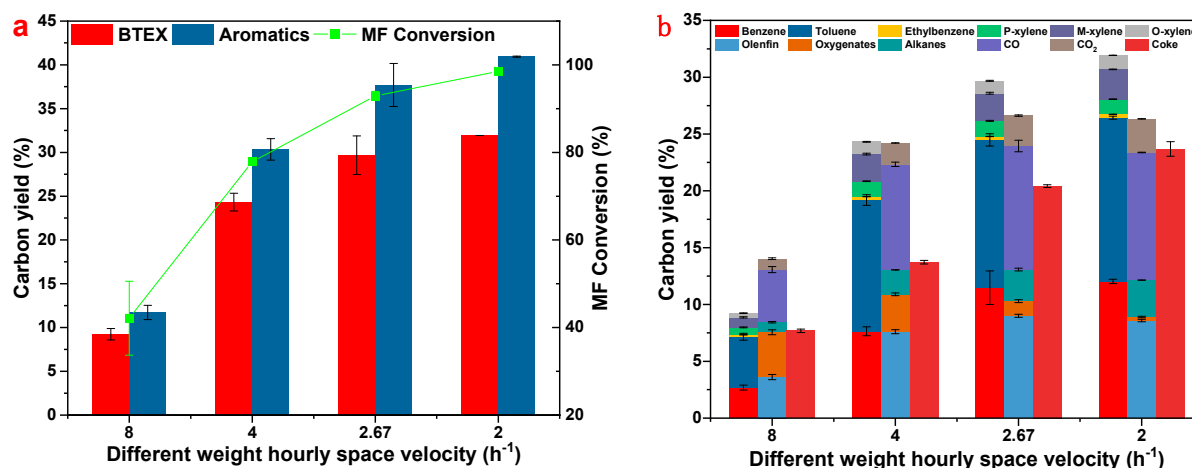


**Figure 3.** Effect of WHSV on the product distribution from CFP of bio-derived MF: (a) carbon yields of BTEX, aromatics, and MF conversion; (b) carbon yields of benzene, toluene, ethylbenzene, xylene, olefins, oxygenates, alkane, CO, CO<sub>2</sub>, and coke. Reaction conditions: 550 °C, catalyst: 2%Fe-ZSM-5, carrier gas flow rate: 120 mL/min, reaction time: 15 min.

#### 2.4. The Structure-Reactivity Relationship of Metal-Modified ZSM-5 during the CFP of MF

The acid sites and shape selectivity of the zeolite microporous structure are key factors determining the catalytic performance of metal-modified ZSM-5 during the CFP of MF. The N<sub>2</sub> adsorption-desorption isotherms and pore size distribution of different catalysts are illustrated in Figure 4; the resulting BET surface area, pore volume, and pore size are tabulated in Table 1. It is well-known that the molecular-sized micropore structure of ZSM-5 catalysts provides spatial restrictions around acid sites that allow for shape-selective catalysis. It can be seen from Table 1 and Figure 4 that the loading of metal species alters the specific surface area and total pore volume since the ZSM-5 was heated to 60 °C in the metal nitrate solution to evaporate the water during the catalyst preparation process. As the Fe loading increases from 0.5 to 4%, the BET surface and total pore volume area of Fe-ZSM-5 first increase and then reach their maximum value at the 2% Fe loading. Larger specific surface area and pore volume are beneficial for the aromatization reaction of MF. The results are in line with those in Figure 2, where 2%Fe-ZSM-5 exhibits the maximum yield of aromatics. It is worth noting that a large number of mesopores are generated when the Fe loading is from 1 to 3%. The mass transfer of reactant, intermediates, and products in zeolite channels can be enhanced by the introduction of a large number of mesopores, thus facilitating the aromatization of MF.

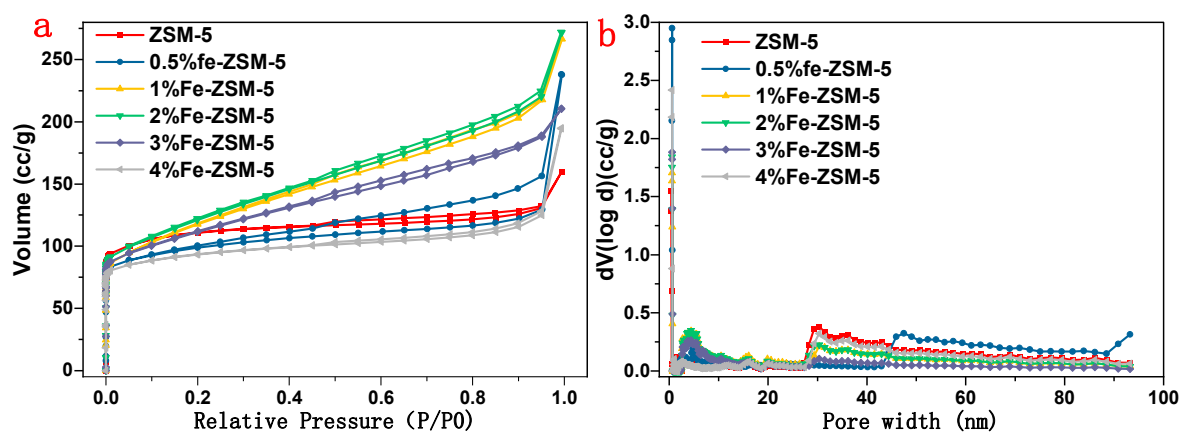


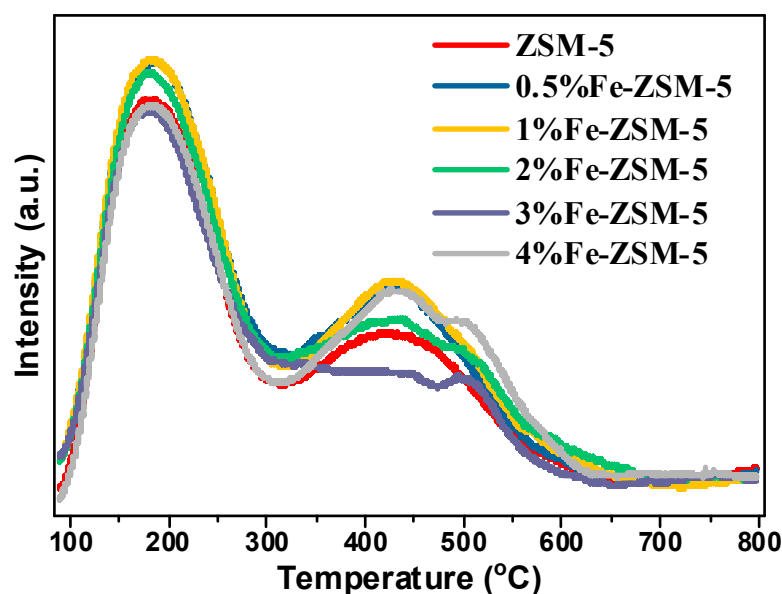
**Figure 4.** N<sub>2</sub> adsorption and desorption isotherms (a) and pore size distribution (b) diagram of different catalysts.

**Table 1.** The BET surface area, pore volume, and pore size of different catalysts.

Catalysts	BET Surface (m <sup>2</sup> /g) <sup>a</sup>	Total Pore Volume (cm <sup>3</sup> /g) <sup>b</sup>	Average Pore Size (nm)	Micropore Volume (cm <sup>3</sup> /g) <sup>c</sup>	Mesopore Volume (cm <sup>3</sup> /g)	Micropore Surface Area (m <sup>2</sup> /g) <sup>c</sup>	External Surface Area (m <sup>2</sup> /g)
ZSM-5	408.0	0.34	3.4	0.14	0.20	336.0	72.0
0.5%Fe-ZSM-5	367.4	0.37	4.0	0.12	0.25	291.5	75.8
1%Fe-ZSM-5	380.2	0.41	4.3	0.07	0.35	113.4	266.7
2%Fe-ZSM-5	423.4	0.42	4.0	0.08	0.35	160.5	262.9
3%Fe-ZSM-5	393.8	0.33	3.3	0.08	0.25	172.2	221.6
4%Fe-ZSM-5	352.3	0.30	3.4	0.13	0.17	309.0	43.3

<sup>a</sup> Calculated by multipoint BET method. <sup>b</sup> Calculated from absorbed volume of nitrogen for a relative pressure  $P/P_0$  of 0.99. <sup>c</sup> Determined by t-plot method.

The acid strength and total acid amount of the different catalysts were measured by NH<sub>3</sub>-TPD, as shown in Figure 5 and Table 2. The two peaks centered at 190 °C and 425 °C correspond to the weak and strong acid sites, respectively. It is obvious that the Fe loading increases the amount of strong acid sites, whereas it decreases the amount of weak acid sites. It is well-accepted that strong acid sites are responsible for the formation of coke, which is consistent with the results in Figure 2, where the Fe loading can promote the formation of coke [32]. The Fe loading significantly improves the total acid amount of ZSM-5, which is beneficial for the formation of aromatics during the CFP of MF. As the Fe loading increases from 0.5 to 4%, the total acid amount of Fe-ZSM-5 first increases and then decreases. The minimum total acid amount of 1149.97 μmol/g is obtained by 3%Fe-ZSM-5.

**Figure 5.** NH<sub>3</sub>-TPD profiles of Fe-ZSM-5 with different Fe loadings.**Table 2.** The acid strength and total acid amount of Fe-ZSM-5 with different Fe loadings.

Catalysts	The First Peak (°C)	The Second Peak (°C)	Amount of Weak Acid Sites (μmol/g)	Amount of Strong Acid Sites (μmol/g)	Total Acid Amount (μmol/g)
ZSM-5	182.50	445.00	827.64	189.08	1016.72
0.5%Fe-ZSM-5	191.277	418.22	783.26	539.58	1322.84
1%Fe-ZSM-5	190.89	426.25	763.26	536.78	1300.04
2%Fe-ZSM-5	188.01	415.39	656.50	546.78	1203.28
3%Fe-ZSM-5	184.95	389.45	614.81	535.16	1149.97
4%Fe-ZSM-5	182.9	444.7	709.90	473.41	1183.31

The Brønsted and Lewis acid sites of Fe-ZSM-5 were determined by Py-FTIR. As shown in Table 3, the Fe loading greatly alters the Brønsted to Lewis (B/L) ratio and the

amount of Brønsted acid sites and Lewis acid sites compared to ZSM-5. An FE loading of 0.5% obviously improves the amount of Brønsted acid sites and Lewis acid sites of ZSM-5. The Fe loading further increases from 0.5 to 3% and the amount of Brønsted acid sites of Fe-ZSM-5 gradually drops, whereas the amount of Lewis acid sites continuously increases. The highest amount of Lewis acid sites (714.27  $\mu\text{mol/g}$ ) and the lowest amount of Brønsted acid sites (435.70  $\mu\text{mol/g}$ ) are obtained by 3%Fe-ZSM-5, which also exhibits the maximum MF conversion of 83.34%. It is speculated the MF conversion is associated with the amount of Lewis acid sites of Fe-ZSM-5. However, the significant decrease in the Brønsted acid sites could result in a reduction in the aromatic yield. Hence, 2%Fe-ZSM-5 with the proper amount of Brønsted and Lewis acid sites provides the highest aromatic yield. The synergistic effect of the Brønsted acid sites and Lewis acid sites is responsible for achieving the efficient aromatization of MF. It is thus concluded that the key to designing an improved zeolite catalyst for MF aromatization is the introduction of large numbers of new Lewis acid sites without a significant loss of Brønsted acid sites in ZSM-5.

**Table 3.** The amount of Brønsted and Lewis acid sites of Fe-ZSM-5.

Zeolite	B/L		Amount of Brønsted Acid Sites ( $\mu\text{mol/g}$ )	Amount of Lewis Acid Sites ( $\mu\text{mol/g}$ )
	Total (150 °C)	Strong (350 °C)		
ZSM-5	1.42	2.07	596.59	420.13
0.5%Fe-ZSM-5	1.62	1.87	817.94	504.90
1%Fe-ZSM-5	1.04	1.17	662.77	637.27
2%Fe-ZSM-5	0.85	1.07	552.86	650.42
3%Fe-ZSM-5	0.61	0.73	435.70	714.27
4%Fe-ZSM-5	1.05	1.36	606.09	577.22

### 3. Materials and Methods

#### 3.1. Materials

MF ( $\text{C}_5\text{H}_6\text{O}$ ,  $\geq 98\%$ ), iron(III) nitrate nonahydrate ( $\text{Fe}(\text{NO}_3)_3 \cdot 9\text{H}_2\text{O}$ ,  $\geq 98.5\%$ ), and gallium nitrate hydrate ( $\text{Ga}(\text{NO}_3)_3 \cdot x\text{H}_2\text{O}$ ,  $\geq 99.9\%$ ) were purchased from Shanghai Macklin Biochemical Co., Ltd. Ammonium heptamolybdate ( $(\text{NH}_4)_6\text{Mo}_7\text{O}_{24} \cdot 4\text{H}_2\text{O}$ ,  $\geq 99.0\%$ ) was obtained from Tianjin Komiou Chemical Reagent Co., Ltd, Tianjin, China. Zinc nitrate hexahydrate ( $\text{Zn}(\text{NO}_3)_2 \cdot 6\text{H}_2\text{O}$ ,  $\geq 99.0\%$ ) was supplied by Guangzhou Chemical Reagent Factory, Guangdong, China. ZSM-5 ( $\text{SiO}_2/\text{Al}_2\text{O}_3 = 25$ ) was acquired from Nankai University Catalyst Plant Co., Ltd., Tianjin, China. The ultrapure water was homemade. All reagents were used directly without further purification.

#### 3.2. Catalyst Preparation

The metal-modified ZSM-5 catalysts were prepared by wet impregnation procedures and termed as xMe-ZSM-5 (x denotes weight ratio of metal to zeolite, x = 0.5%, 1%, 2%, 3%, 4%; Me means metal, Me = Mo, Zn, Ga, or Fe). In total, 10 g of ZSM-5 zeolite was impregnated in a 100 mL metal nitrate solution at room temperature and then rotary-evaporated at 60 °C. Subsequently, the samples were dried at 105 °C for 12 h and then calcined at 550 °C for 5 h. In the end, all of the catalysts, including raw ZSM-5, were pelleted, crushed, and sieved into 40–60 mesh for further catalytic assessment.

#### 3.3. CFP Experiments

The conversion of bio-derived furans was conducted in a continuous fixed bed reactor, as shown in Figure 6. The fixed reactor was built from a 17 mm inner diameter quartz tube. The sieved ZSM-5 particles with a size of 0.25–0.425 mm were held in the reactor by quartz beads and quartz wool. Nitrogen (99.999%) was used as a purge gas to remove the air in the fixed bed reactor, while argon (99.999%) was used as a carrier gas for the internal standard of gas volume. The purge gas was set to 200 mL/min using a mass flow meter, and the carrier gas was set to 120 mL/min. The MF was introduced into

the argon stream using a constant flow HPLC piston pump (STI 501, Hangzhou Saizhi Technology Co., Ltd, Hangzhou, China.). For a typical run, the flow rate of the mixtures was adjusted to 4.0 g/h, and 1.0 g of catalysts were used in the catalyst bed. All of the runs were performed at atmospheric pressure. A condenser at  $-40\text{ }^{\circ}\text{C}$  and two-stage gas washing bottles using cyclohexane as a solvent (held at  $0\text{ }^{\circ}\text{C}$ ) were used to trap the liquid products. After the reactions, the condenser and gas-washing bottles were washed with cyclohexane. The liquid products in the cyclohexane were analyzed and quantified by a TRACE 1300 gas chromatograph connected with a QD-300 mass spectrometer (GC-MS) (Thermo Fisher Scientific, Cleveland, OH, USA). The GC column was an Agilent HP-5 (30 m length, 0.25 mm internal diameter, and 0.25  $\mu\text{m}$  film thickness). The gas phase products were collected with airbags and analyzed by GC (Agilent 7890A, Agilent Technologies, Inc, Santa Clara, CA, USA). The GC column was an Agilent 113-4362 GS-GASPRO (60 m length, 0.32 mm internal diameter). The coke yield was obtained by measuring the carbon content of the spent catalyst.

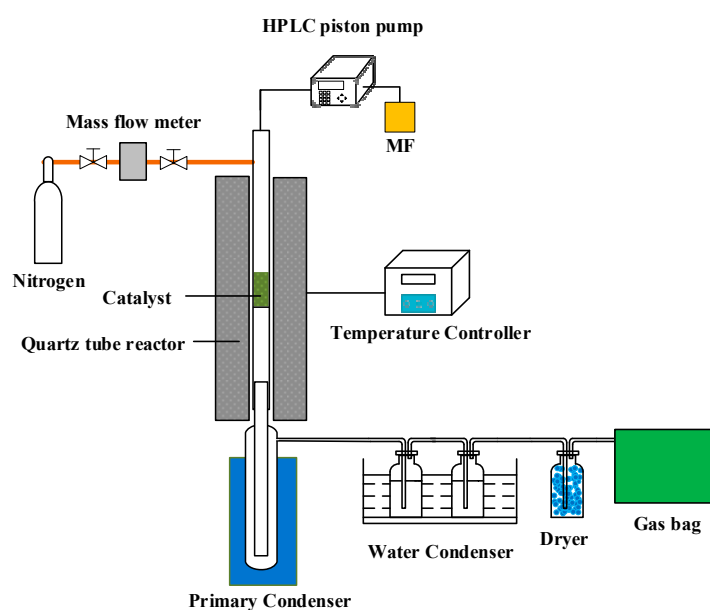


**Figure 6.** The schematic diagram of the fixed bed for CFP of MF.

### 3.4. Characterization

The textural properties of catalysts were determined by  $\text{N}_2$  adsorption-desorption isotherms (Autosorb-iQ-2, Quantachrome). Before the test, the sample was degassed under a vacuum at  $300\text{ }^{\circ}\text{C}$  for 10 h. The  $\text{NH}_3$ -TPD analysis of different catalysts was conducted on an AutoChem II 2920 (Micromeritics) chemisorption analyzer following a TPD method. For each run, the sample was heated up to  $300\text{ }^{\circ}\text{C}$  at a rate of  $10\text{ }^{\circ}\text{C}/\text{min}$  and kept for 2 h in a He flow to remove adsorbed impurities. Then, the sample was cooled down to  $90\text{ }^{\circ}\text{C}$  for the adsorption of  $\text{NH}_3$ . After flushing with He for 1 h to remove physically adsorbed  $\text{NH}_3$ , the  $\text{NH}_3$  desorption signal was detected using a TCD detector from  $90\text{ }^{\circ}\text{C}$  to  $800\text{ }^{\circ}\text{C}$  with a ramp of  $10\text{ }^{\circ}\text{C}/\text{min}$ . The Fourier transform infrared spectroscopy of pyridine adsorption (Py-FTIR) of different catalysts was obtained by a Thermo Nicolet Nexus 6700 FT-IR spectrometer equipped with a liquid nitrogen-cooled MCT detector. The wafers (diameter 13 mm) were purged in the IR cell at  $400\text{ }^{\circ}\text{C}$  for 2 h under a vacuum and then cooled down to room temperature for pyridine adsorption. Py-IR spectra were recorded over 32 scans at a resolution of  $4\text{ cm}^{-1}$  in the range of  $1700$  to  $1400\text{ cm}^{-1}$  at  $150$  and  $350\text{ }^{\circ}\text{C}$ . The Brønsted/Lewis acid (B/L) ratio was calculated as follows:  $\text{B/L} = 1.88\text{IA}(\text{B})/1.42\text{IA}(\text{L})$  ( $\text{IA}(\text{L}, \text{B})$ ,  $\text{IA}$  = integrated absorbance of L or B band).

### 3.5. Methods of Data Processing

The MF conversion, the carbon yields of aromatics, oxygenates, coke, and noncondensable gases (alkanes, olefins, CO, and CO<sub>2</sub>), and aromatic selectivity were defined as follows:

$$\text{MF conversion} = \left(1 - \frac{\text{Moles of carbon of MF in the product}}{\text{Moles of carbon in feedstocks}}\right) \times 100\%$$

$$\text{Aromatic yield} = \frac{\text{Moles of carbon in aromatic products}}{\text{Moles of carbon in feedstocks}} \times 100\%$$

$$\text{Coke yield} = \frac{\text{Moles of carbon in spent catalysts}}{\text{Moles of carbon in feedstocks}} \times 100\%$$

$$\text{Noncondensable gas yield} = \frac{\text{Moles of carbon in noncondensable gas}}{\text{Moles of carbon in feedstocks}} \times 100\%$$

$$\text{Aromatic selectivity} = \frac{\text{Moles of carbon in specific aromatic species}}{\text{Total Moles of carbon in all aromatic species}} \times 100\%$$

## 4. Conclusions

It is demonstrated that the introduction of Zn, Mo, Fe, and Ga on ZSM-5 evidently improves the MF conversion and the aromatic yield during the CFP of MF. Among the four types of metal-modified ZSM-5 catalysts, 1%Fe-ZSM-5 exhibits the highest MF conversion, while Ga-ZSM-5 affords higher aromatic yields. It is found that 2% is the optimal Fe loading for maximizing the aromatic yield during the CFP of MF over Fe-ZSM-5. The optimal aromatic yield of 40.03% is achieved by 2%Fe-ZSM-5 at a WHSV of 2 h<sup>-1</sup>. The NH<sub>3</sub>-TPD and Py-FTIR characterization prove that the synergistic effect of Brønsted acid sites and Lewis acid sites is the key to achieving the efficient aromatization of MF. The introduction of large numbers of new Lewis acid sites without a significant loss of Brønsted acid sites on the ZSM-5 catalyst is the guideline for the rational design of an improved zeolite catalyst for the CFP of biomass and its derived furans.

**Author Contributions:** Conceptualization, K.Z. and A.Z.; Methodology, Z.Z.; Validation, S.K.; Formal analysis, S.X.; Investigation, C.W., Y.C. and K.Z.; Resources, H.L.; Data curation, S.X.; Writing—original draft, S.X.; Writing—review and editing, A.Z.; Supervision, H.L.; Funding acquisition, K.Z. All authors have read and agreed to the published version of the manuscript.

**Funding:** This research was funded by the National Key R&D Program of China (Grant 2017YFE0124200), the National Natural Science Foundation of China (Grants 51876208 and 51776209), the Key Research and Development Program of Guangzhou (202206010122), and the Youth Innovation Promotion Association, CAS (2019341).

**Data Availability Statement:** Not applicable.

**Acknowledgments:** The authors acknowledge the National Key R&D Program of China (Grant 2017YFE0124200), the National Natural Science Foundation of China (Grants 51876208 and 51776209), the Key Research and Development Program of Guangzhou (202206010122), and the Youth Innovation Promotion Association, CAS (2019341), for their financial support of this work.

**Conflicts of Interest:** The authors declare no conflict of interest.

## References

1. Zhao, N.; You, F.Q. Can renewable generation, energy storage and energy efficient technologies enable carbon neutral energy transition? *Appl. Energy* **2020**, *279*, 115889. [CrossRef]
2. Van Meerbeek, K.; Muys, B.; Hermy, M. Lignocellulosic biomass for bioenergy beyond intensive cropland and forests. *Renew. Sustain. Energy Rev.* **2019**, *102*, 139–149. [CrossRef]
3. Rezaei, P.S.; Shafaghat, H.; Daud, W.M.A.W. Production of green aromatics and olefins by catalytic cracking of oxygenate compounds derived from biomass pyrolysis: A review. *Appl. Catal. A: Gen.* **2014**, *469*, 490–511. [CrossRef]
4. Che, Q.; Yang, M.; Wang, X.; Chen, X.; Chen, W.; Yang, Q.; Yang, H.; Chen, H. Aromatics production with metal oxides and ZSM-5 as catalysts in catalytic pyrolysis of wood sawdust. *Fuel Process. Technol.* **2019**, *188*, 146–152. [CrossRef]

5. Butler, E.; Devlin, G.; Meier, D.; McDonnell, K. A review of recent laboratory research and commercial developments in fast pyrolysis and upgrading. *Renew. Sustain. Energy Rev.* **2011**, *15*, 4171–4186. [[CrossRef](#)]
6. Bridgwater, A.V. Review of fast pyrolysis of biomass and product upgrading. *Biomass Bioenergy* **2012**, *38*, 68–94. [[CrossRef](#)]
7. Zhang, X.; Yuan, Z.; Yao, Q.; Zhang, Y.; Fu, Y. Catalytic fast pyrolysis of corn cob in ammonia with Ga/HZSM-5 catalyst for selective production of acetonitrile. *Bioresour. Technol.* **2019**, *290*, 121800. [[CrossRef](#)]
8. Iliopoulou, E.F.; Triantafyllidis, K.S.; Lappas, A.A. Overview of catalytic upgrading of biomass pyrolysis vapors toward the production of fuels and high-value chemicals. *WIREs Energy Environ.* **2018**, *8*, e322. [[CrossRef](#)]
9. Potera, G.T. *The Effects of Benzene, Toluene and Ethylbenzene on Several Important Members of the Estuarine Ecosystem*; Lehigh University: Bethlehem, PA, USA, 1975.
10. Sun, R.; Shen, S.; Zhang, D.; Ren, Y.; Fan, J. Hydrofining of coal tar light oil to produce high octane gasoline blending components over  $\gamma$ -Al<sub>2</sub>O<sub>3</sub>- and  $\eta$ -Al<sub>2</sub>O<sub>3</sub>-supported catalysts. *Energy Fuels* **2015**, *29*, 7005–7013. [[CrossRef](#)]
11. Li, X.; Su, L.; Wang, Y.; Yu, Y.; Wang, C.; Li, X.; Wang, Z. Catalytic fast pyrolysis of Kraft lignin with HZSM-5 zeolite for producing aromatic hydrocarbons. *Front. Environ. Sci. Eng.* **2012**, *6*, 295–303. [[CrossRef](#)]
12. Kim, J.-Y.; Lee, J.H.; Park, J.; Kim, J.K.; An, D.; Song, I.K.; Choi, J.W. Catalytic pyrolysis of lignin over HZSM-5 catalysts: Effect of various parameters on the production of aromatic hydrocarbon. *J. Anal. Appl. Pyrolysis* **2015**, *114*, 273–280. [[CrossRef](#)]
13. Thiyagarajan, S.; Genuino, H.C.; van der Waal, J.C.; de Jong, E.; Weckhuysen, B.M.; van Haveren, J.; Bruijninx, P.C.; van Es, D.S. A Facile Solid-Phase Route to Renewable Aromatic Chemicals from Biobased Furans. *Angew. Chem. Int. Ed. Engl.* **2016**, *55*, 1368–1371. [[CrossRef](#)] [[PubMed](#)]
14. Li, G.; Yan, L.; Zhao, R.; Li, F. Improving aromatic hydrocarbons yield from coal pyrolysis volatile products over HZSM-5 and Mo-modified HZSM-5. *Fuel* **2014**, *130*, 154–159. [[CrossRef](#)]
15. Sun, L.; Zhang, X.; Chen, L.; Zhao, B.; Yang, S.; Xie, X. Comparison of catalytic fast pyrolysis of biomass to aromatic hydrocarbons over ZSM-5 and Fe/ZSM-5 catalysts. *J. Anal. Appl. Pyrolysis* **2016**, *121*, 342–346. [[CrossRef](#)]
16. Fanchiang, W.-L.; Lin, Y.-C. Catalytic fast pyrolysis of furfural over H-ZSM-5 and Zn/H-ZSM-5 catalysts. *Appl. Catal. A Gen.* **2012**, *419–420*, 102–110. [[CrossRef](#)]
17. Uslamin, E.A.; Kosinov, N.A.; Pidko, E.A.; Hensen, E.J.M. Catalytic conversion of furanic compounds over Ga-modified ZSM-5 zeolites as a route to biomass-derived aromatics. *Green Chem.* **2018**, *20*, 3818–3827. [[CrossRef](#)]
18. Li, W.; Wang, D.; Zhu, Y.; Chen, J.; Lu, Y.; Li, S.; Zheng, Y.; Zheng, Z. Efficient ex-situ catalytic upgrading of biomass pyrolysis vapors to produce methylfurans and phenol over bio-based activated carbon. *Biomass- Bioenergy* **2020**, *142*, 105794. [[CrossRef](#)]
19. Zheng, A.; Zhao, Z.; Chang, S.; Huang, Z.; Zhao, K.; Wu, H.; Wang, X.; He, F.; Li, H. Maximum synergistic effect in the coupling conversion of bio-derived furans and methanol over ZSM-5 for enhancing aromatic production. *Green Chem.* **2014**, *16*, 2580–2586. [[CrossRef](#)]
20. Chang, C.-C.; Green, S.K.; Williams, C.L.; Dauenhauer, P.J.; Fan, W. Ultra-selective cycloaddition of dimethylfuran for renewable p-xylene with H-BEA. *Green Chem.* **2014**, *16*, 585–588. [[CrossRef](#)]
21. Qi, X.; Fan, W. Selective Production of Aromatics by Catalytic Fast Pyrolysis of Furan with In Situ Dehydrogenation of Propane. *ACS Catal.* **2019**, *9*, 2626–2632. [[CrossRef](#)]
22. Cheng, Y.-T.; Huber, G.W. Production of targeted aromatics by using Diels–Alder classes of reactions with furans and olefins over ZSM-5. *Green Chem.* **2012**, *14*, 3114–3125. [[CrossRef](#)]
23. Ni, L.; Xin, J.; Jiang, K.; Chen, L.; Yan, D.; Lu, X.; Zhang, S. One-Step Conversion of Biomass-Derived Furans into Aromatics by Brønsted Acid Ionic Liquids at Room Temperature. *ACS Sustain. Chem. Eng.* **2018**, *6*, 2541–2551. [[CrossRef](#)]
24. Do, P.T.M.; McAtee, J.R.; Watson, D.A.; Lobo, R.F. Elucidation of Diels–Alder Reaction Network of 2,5-Dimethylfuran and Ethylene on HY Zeolite Catalyst. *ACS Catal.* **2013**, *3*, 41–46. [[CrossRef](#)] [[PubMed](#)]
25. Williams, C.L.; Chang, C.-C.; Do, P.; Nikbin, N.; Caratzoulas, S.; Vlachos, D.G.; Lobo, R.F.; Fan, W.; Dauenhauer, P.J. Cycloaddition of Biomass-Derived Furans for Catalytic Production of Renewable p-Xylene. *ACS Catal.* **2012**, *2*, 935–939. [[CrossRef](#)]
26. Espindola, J.S.; Gilbert, C.J.; Perez-Lopez, O.; Trierweiler, J.O.; Huber, G.W. Conversion of furan over gallium and zinc promoted ZSM-5: The effect of metal and acid sites. *Fuel Process. Technol.* **2020**, *201*, 106319. [[CrossRef](#)]
27. Cheng, Y.-T.; Huber, G.W. Chemistry of Furan Conversion into Aromatics and Olefins over HZSM-5: A Model Biomass Conversion Reaction. *ACS Catal.* **2011**, *1*, 611–628. [[CrossRef](#)]
28. Cheng, Y.-T.; Jae, J.; Shi, J.; Fan, W.; Huber, G.W. Production of Renewable Aromatic Compounds by Catalytic Fast Pyrolysis of Lignocellulosic Biomass with Bifunctional Ga/ZSM-5 Catalysts. *Angew. Chem. Int. Ed.* **2012**, *51*, 1387–1390. [[CrossRef](#)]
29. Wang, C.; Si, Z.; Wu, X.; Lv, W.; Bi, K.; Zhang, X.; Chen, L.; Xu, Y.; Zhang, Q.; Ma, L. Mechanism study of aromatics production from furans with methanol over zeolite catalysts. *J. Anal. Appl. Pyrolysis* **2019**, *139*, 87–95. [[CrossRef](#)]
30. Teixeira, I.F.; Lo, B.T.W.; Kostetsky, P.; Stamatakis, M.; Ye, L.; Tang, C.C.; Mpourmpakis, G.; Tsang, S.C.E. From Biomass-Derived Furans to Aromatics with Ethanol over Zeolite. *Angew. Chem. Int. Ed.* **2016**, *55*, 13061–13066. [[CrossRef](#)]
31. Zhang, H.; Wang, Y.; Shao, S.; Xiao, R. An experimental and kinetic modeling study including coke formation for catalytic pyrolysis of furfural. *Combust. Flame* **2016**, *173*, 258–265. [[CrossRef](#)]
32. Wang, B.; Manos, G. Role of strong zeolitic acid sites on hydrocarbon reactions. *Ind. Eng. Chem. Res.* **2008**, *47*, 2948–2955. [[CrossRef](#)]